Research Article

Climacteric Respiration and Fatty and Amino Acids Drive Volatile Ester Biosynthesis in Monthong Durian Aril during Fruit Maturation

Duangkamol Tungsatitporn
Program in Bio-Industrial Technology, Department of Agro-Industrial, Food, and Environmental Technology, Faculty of Applied Science, King Mongkut's University of Technology North Bangkok, Bangkok, Thailand

Chalermchai Wongs-Aree*
Division of Postharvest Technology, School of Bioresources and Technology, King Mongkut's University of Technology Thonburi, Bangkok, Thailand
Postharvest Technology Innovation Center, Science, Research and Innovation Promotion and Utilization Division, Office of the Ministry of Higher Education, Science, Research and Innovation, Bangkok, Thailand

Bryl I. Manigo
Division of Postharvest Technology, School of Bioresources and Technology, King Mongkut's University of Technology Thonburi, Bangkok, Thailand

Wattana Aschariyaphotha
Thai Traditional Biological Science Program, Faculty of Science and Technology, Valaya Alongkorn Rajabhat University under the Royal Patronage, Pathum Thani, Thailand

Kitti Bodhipadma and Sompoch Noichinda*
Department of Agro-Industrial, Food, and Environmental Technology, Faculty of Applied Science, King Mongkut's University of Technology North Bangkok, Bangkok, Thailand

* Corresponding author. E-mail: chalermchai.won@kmutt.ac.th; sompoch.n@sci.kmutnb.ac.th
DOI: 10.14416/j.asep.2026.02.006
Received: 22 August 2025; Revised: 15 October 2025; Accepted: 5 November 2025; Published online: 5 February 2026

Abstract
The distinctive flavor of durian fruit is increasingly characterized, yet the metabolic pathways during ripening are not fully understood. This study investigated the volatile dynamics in ripening Monthong durian, revealing clear correlations between ripening stages and aroma compound production. Fruit ethylene production peaked one day after the first climacteric peak, initiating the second climacteric peak, pulp softening, and ester and sulfur-containing volatile emission. Ethanethiol, ethyl-2-methyl butanoate, ethyl-2-methyl propanoate, ethyl butanoate, and ethyl hexanoate dominate the odor, along with somewhat fermented ethanol and acetaldehyde. Ethanethiol and ethyl-2-methylbutanoate intensely elevated during late ripening, although D-limonene prevailed early. Short-chain fatty acid esters were performed early on, whereas branched-chain amino acid esters increased significantly in overripe fruit. Valine, leucine, isoleucine, and methionine increased 1.07–1.29-fold from unripe to overripe, while cysteine and glutamic acid decreased 1.11–1.25-fold. Propionic acid (C_3) was found throughout, whereas acetic acid (C_2) increased significantly 22-fold from ripe to overripe stages. The main free fatty acids throughout maturation were palmitic ($C_{16:0}$) and Z-9-oleic ($C_{18:1}$). Linoleic acid ($C_{18:2}$) fell by 25% from unripe to ripe pulp, but linolenic acid ($C_{18:3}$) increased 44%. Lipoxygenase activity increased throughout maturation, notably in overripe pulp, promoting fatty acid breakdown and volatile generation. From unripe to overripe, aldehyde dehydrogenase and alcohol acetyltransferase activity increased 1.6- and 1.8-fold, respectively. These findings demonstrate that the coordinated metabolism of fatty acids and amino acids, mediated by key enzymes, drives ester biosynthesis during durian fruit ripening.

Keywords: Alcohol acetyltransferase, Double climacteric respiration, *Durio zibethinus* L., Ester volatiles, Flavor, Fruit ripening

1 Introduction

Durian (*Durio zibethinus* L.), an economically significant tropical fruit native to Southeast Asia, has experienced rising global demand, particularly in China [1]. Among its many cultivars, Monthong is Thailand's most commercially important, dominating both domestic and international markets due to its high economic value, favorable agronomic traits, and strong consumer appeal [2], particularly its extended shelf life, supporting long-distance export. Thailand exports approximately 75% of its total durian production, with China accounting for 97% of these exports. In Chinese wholesale markets, Monthong holds the commercial majority of all durians sold [3]. Thai durians exported to China are commonly treated with ethephon, an ethylene-releasing agent that induces ripening within 7–10 days during transit at 15 °C. These fruits typically arrive ripe and are promptly distributed [4], although logistical delays may disrupt uniform ripening. A promising alternative may involve exporting untreated mature green durians for post-arrival ripening, allowing for improved market responsiveness and quality control. During ripening, durian pulp undergoes metabolic changes involving volatiles [5], [6], fatty acids [7], amino acids [8], carotenoids [9], and bioactive compounds [8], [10].

Fruit aroma is a pivotal factor in quality perception and consumer acceptance, shaped by a complex array of volatile organic compounds (VOCs) that define each fruit's aromatic profile. These VOCs include esters, ketones, aldehydes, lactones, alcohols, and terpenes, with the specific composition varying across fruit species [11]. Durian, a widely recognized tropical fruit, is renowned for its potent and intricate aroma, predominantly composed of esters, aldehydes, and sulfur-containing compounds. Studies have shown that esters and sulfur volatiles are the principal contributors to durian's signature flavor [5], [6], [12]. While esters impart fruity notes, sulfur-containing compounds intensify and synergize the characteristic durian scent [11], [13].

Comparative analyses of durian cultivars from Thailand (Monthong), Malaysia (D2), Indonesia (Ajimah), and the Philippines (Puyat) have identified at least 15 major volatile organic compounds (VOCs) in ripe pulp. These compounds include 9 esters: ethyl propanoate, methyl-2-methyl butanoate, ethyl butanoate, ethyl-2-methyl butanoate, propyl-2-methyl butanoate, ethyl hexanoate, ethyl heptanoate, ethyl octanoate, ethyl decanoate and 6 sulfur compounds: ethanethiol, 1-propanethiol, diethyl disulfide, diethyl trisulfide, 1,1-bis (ethylthio) ethane, and 3,5-dimethyl-1,2,4-trithiolane [14]. Subsequent studies on the primary VOCs in 4 Thai durian varieties, Chanthaburi 1 (a low smell), Chanee (a strong smell), Monthong (a mild aroma), and Kan Yao (a mild smell), revealed that ripe pulp primarily contains ethyl-2-methylbutanoate and ethyl hexanoate, both associated with apple-like aromas. Sulfur-containing volatiles, such as diethyl disulfide and trisulfide, contribute to garlic and onion-like odors, while 3,5-dimethyl-1,2-thrithiolane evokes a sulfurous onion scent [5]. In combination with esters, these compounds generate durian's potent aroma. Notably, the absence of sulfides could yield a fruit profile resembling ripe apple and pineapple. The biosynthesis of esters is largely controlled by the enzyme alcohol acyltransferase (AAT), which is considered rate-limiting in many fruit species. AAT activity is ripening-specific and ethylene-dependent, catalyzing the final step of ester formation from alcohol and acyl-CoA substrates [15]–[17]. In durian, numerous volatile esters are synthesized during ripening [14]. However, the complete biochemical pathways that supply these alcohol and acyl-CoA precursors from the metabolism of fatty acids, amino acids, and carboxylic acids are not fully elucidated. These upstream pathways likely involve key enzymes such as lipoxygenase (LOX), alcohol dehydrogenase (ADH), and aldehyde dehydrogenase (ALDH).

A comprehensive understanding of these biochemical precursors and enzymatic mechanisms is essential for managing aroma development and ensuring consistent fruit quality. This is particularly relevant given the logistical challenges in the durian supply chain. This study hypothesizes that the production of specific aroma volatiles results from dynamic changes in the pools of fatty acids, amino acids, and carboxylic acids, and the corresponding activities of LOX, ADH, ALDH, and AAT. Therefore, this study aimed to investigate the metabolic pathways of ester formation by analytically correlating dynamic changes in Monthong durian pulp across three ripening stages (unripe, ripe, and overripe). By characterizing the biochemical dynamics and correlating the volatile profile with precursor substrates and enzyme activities, this research sought to clarify the molecular basis of durian aroma.

2 Materials and Methods

2.1 *Plant material and sample preparation*

Monthong durian fruits were collected from a commercial orchard in Chanthaburi Province, Thailand, in June 2022. Each fruit weighed approximately 3–4 kg and was harvested at 115–120 days post-hand pollination (mature unripe stage) and delivered to a laboratory in Bangkok within 5 h via a refrigerated truck. Fruits were ripened naturally under ambient conditions (25–36 °C, 50–68% relative humidity). In total 18 fruits, three stages of fruit maturation were identified for analysis: unripe fruit (initial stage: IS), ripe fruit (~9 days post-IS, characterized by the emission of a distinct aroma), and overripe stage (~14 days post-IS, marked by clear cracking and a star-like appearance of the pericarp). Each stage consisted of three biological replicates, with three fruits per replicate. Fruit and pulp characteristics at each stage are shown in Figure S1. The same fruit samples were used for volatile-related analyses, including volatile compounds (Section 2.3), substrate precursors (fatty acids and amino acids, Section 2.4), and enzyme activities (Section 2.5).

2.2 *Physical quality analysis*

2.2.1 Pulp color

Pulp color was assessed using a Minolta Chromameter (CR-300, Minolta Co., Japan). Samples from the center of durian pods were finely chopped and placed into the measurement chamber. The color was recorded in the CIELAB color space as L* (lightness), a* (red/green), and b* (yellow).

2.2.2 Pulp firmness

Pulp firmness was evaluated using a Texture Analyzer (TA-XT 21) equipped with a 2 mm cylindrical stainless-steel probe (SMS P/2). Each durian pod was evaluated at three positions (left, center, right). The probe penetrated 5 mm into the pulp at a constant rate of 1.5 mm·s^{-1}. Firmness values were expressed in Newtons (N).

2.2.3 Respiration and ethylene production

Fruit respiration and ethylene (ET) production were determined following Nguyen *et al*. [18]. A single fruit was sealed in a 5,200-mL airtight plastic container for 1 h at 25 °C (80–85% RH). Headspace gas (1 mL) was sampled and analyzed using a Shimadzu GC-2014 (Kyoto, Japan) equipped with a Porapak Q 80/100 column (3.0 m length×3.00 mm ID). CO_2 was detected via a thermal conductivity detector (TCD, Channel 1), and ET via a flame ionization detector (FID, Channel 2). Helium served as the carrier gas (flow rate: 35 mL·min^{-1}). Injector, column, and detector temperatures were maintained at 120 °C, 90 °C, and 230 °C, respectively. Respiration rate was expressed as mg CO_2·kg^{-1}·h^{-1}, and ET production as μL·kg^{-1}·h^{-1}.

2.3 *Volatile compound and aroma profile analysis in durian pulp*

2.3.1 Volatile compound analysis

Volatile compounds in Monthong durian pulp were analyzed across three ripening stages using headspace (HS) sampling and GC–MS [5].

Identification of volatile compounds

Five grams of finely ground durian pulp were transferred into a 20-mL HS vial, with 10 μL thiophene added as an internal standard (IS). Vials were sealed and analyzed using a GC–MS system (Nexis GC-2030 MS, Shimadzu, Japan) fitted with an HP-5MS column (30 m × 0.32 mm ID, 0.5 μm film thickness). Injection was performed in splitless mode at 200 °C. The oven temperature was programmed at 50 °C for 1 min, ramped to 120 °C, then to 250 °C at 10 °C·min^{-1}. Helium was the carrier gas (2 mL·min^{-1}; pressure: 15.9 psi). Volatile compounds were identified by matching spectra to the Wiley 2000 Library (≥80% similarity).

Quantification of volatile compounds

Compound concentrations were quantified relative to the internal standard. Calculations were based on the known thiophene concentration (0.5 μg·mL^{-1}), sample weight, and added standard volume (10 μL). The volatile content (ng thiophene·g^{-1} FW) was determined using the following equation:

$$\text{Volatile content} = \frac{\text{Volatile peak area} \times \text{Amount of IS (ng)}}{\text{IS peak area} \times \text{Sample weight (g)}}$$

Where, IS = Internal standard

2.3.2 Odor characterization

Odor activity values (OAVs)
OAVs of volatile compounds were calculated following Aschariyaphotha *et al*. [5], using the formula:

$$\text{OAV} = \frac{\text{Volatile concentration}}{\text{Odor threshold value}}$$

A compound with an OAV > 1 was considered a likely contribution to the overall aroma; compounds with the highest OAVs were considered key odorants.

Odor profile classification
Volatile compounds identified in Section 2.3.1 were cross-referenced with scientific databases and literature to categorize them into odor groups: fruity esters, green-smelling aldehydes, pungent sulfur volatiles, and others. This classification reflects the sensory diversity of durian pulp [11], [13].

2.4 *Chemical substrate analysis*

2.4.1 Free fatty acid composition

The extraction method was adapted from Phutdhawong *et al*. [7]. Durian pulp (~2 g) was dried at 105 °C for 30 h, then ground into a fine powder. One gram of the dried sample was wrapped in fat-free filter paper and placed in a 25×80 mm extraction thimble. Lipid extraction was performed using a Soxhlet apparatus with 80 mL of petroleum ether (boiling range: 40–60 °C) at 105 °C. The lipid extract was dried at 105 °C for 2 h and stored in a desiccator. One gram of fat extract was combined with 20 mL 99.8% methanol and 0.05 g sodium chloride. The solution was extensively agitated and transesterified overnight. The resulting fatty acid methyl esters (FAMEs) were separated, washed with dichloromethane (99.5%) and distilled water, and concentrated to 2 mL for GC-MS analysis, following the protocol of Li *et al*. [19].

2.4.2 Short-chain carboxylic acid composition

The protocol was adapted from Lenti *et al*. [20]. One gram of the blended durian sample was combined with 2 mL of distilled water and thoroughly mixed. Subsequently, 2.4 g of $NaH_2PO_4.2H_2O$ was added and the mixture was vortexed for 1 min. Thereafter, 1.6 mL of ethyl acetate was introduced, followed by vortexing for 3 min. The mixture was then centrifuged at 12,000×g for 5 min. The upper supernatant was collected and supplemented with an internal standard, crotonic acid, to achieve a final concentration of 20 ppm. A 1 µL aliquot of the prepared solution was injected into a GC-FID system (SHIMADZU; Nexis GC-2030) equipped with a CP-Wax 52 CB Column (50 m×0.32 mm ID). Helium was utilized as the carrier gas at a flow rate of 150 kPa. The gas chromatography conditions were as follows: the injection temperature was set to 250 °C; the oven temperature was initially 120 °C, then increased at a rate of 10 °C·min^{-1} to 200 °C, where it was held for 5 min. The FID detector temperature was maintained at 280 °C.

2.4.3 Amino acid composition

The protocol was adapted from Amid *et al*. [21]. Durian pulp (0.25 g) was acid-hydrolyzed with 6 N HCl, digested at 110 °C for 24 h, and vacuum-dried. Then, 10 mL 100 mM phenylisothiocyanate (PITC) was added to derivatize free amino acids. The analysis used two buffer solutions as the mobile phase: Buffer A, 0.1 M ammonium acetate (pH 6.5), and Buffer B, 44:46:10 acetonitrile, methanol. A 40 µL sample solution aliquot was sent to an HPLC system (Agilent 1260 Infinity II, Agilent Technologies, USA) at a flow rate of 1 mL·min^{-1}. A reverse-phase TC-C_{18} column (Zorbax, 4.6 mm×250 mm, 5 µm; Agilent Technologies, USA) was used for separation at 40 °C. Chromatograms were produced at 254 nm.

2.5 *Enzyme activity assays*

For all enzyme assays, protein concentration in the crude extract was determined using the Bradford method [22] with bovine serum albumin (BSA) as the standard.

2.5.1 Lipoxygenase (LOX) activity

Durian pulp (3 g) was fragmented and ground with a chilled mortar and pestle at 4 °C. The homogenate was mixed with 6 mL of 50 mM sodium phosphate buffer (pH 7.0) and centrifuged at 10,000×g for 15 min at 4 °C. The supernatant was collected as the crude enzyme extract. Following Sirikesorn *et al*. [23], lipoxygenase activity was assessed using a linoleic acid substrate. The substrate solution was prepared by mixing 0.5 g linoleic acid, 0.5 g Tween-20, and 3 mL of 0.2 M phosphate buffer (pH 6.5), adjusted to 25 mL with distilled water and clarified with 2 N sodium hydroxide. For the assay, 20 µL enzyme extract was

mixed with 20 µL of linoleic acid solution and incubated at room temperature for 3 min. Absorbance was measured at 234 nm using a spectrophotometer. One unit of LOX activity corresponded to an increase in absorbance of 0.1 per min. Activity was expressed in unit·mg^{-1} protein.

$$\text{LOX activity} = \frac{(\text{Sample absorbance} - \text{Blank absorbance})}{(0.1) \times \text{protein content}}$$

2.5.2 *Aldehyde dehydrogenase (ALDH) activity*

Analysis of ALDH enzyme activity was adapted from Meguro *et al*. [24]. Durian pulp (1.5 g) was ground at 4 °C. The ground pulp was transferred into a microcentrifuge tube containing 2 mL of extraction buffer (pH 8.0). The extraction buffer was prepared by combining the following components: 150 mM Tris-HCl (2.3646 g), 25 mL of 25% glycerol (v/v), 2 g of 2% polyvinylpyrrolidone, 0.8 mL of 0.8% L-mercaptoethanol, 0.077 g of 5 mM dithiothreitol, and 0.5 mL of 0.5% Triton X-100 (v/v). The mixture was filtered and centrifuged at 23,000×g for 15 min at 4 °C. A reaction buffer was prepared using 100 mM sodium phosphate buffer (pH 8.5) composed of 14.196 g of buffer salts. The buffer was supplemented with 0.0431 g of NAD^+ to achieve a concentration of 1.3 mM and 0.04405 g of acetaldehyde to reach a final concentration of 100 µM. Enzyme extract (100 µg) was added and the reaction was initiated with substrate addition. The formation of NADH was monitored at 340 nm. One unit of ALDH activity was defined as an increase in absorbance of 0.1 per minute, and activity was expressed in unit·mg^{-1} protein.

$$\text{ALDH activity} = \frac{\text{Sample absorbance} - \text{Blank absorbance}}{(0.1) \times \text{protein content}}$$

2.5.3 *Alcohol dehydrogenase (ADH) activity*

Analysis of ADH enzyme assay was adapted from Okamura *et al*. [25]. Pulp (1.5 g) was ground at 4 °C and homogenized in 2 mL extraction buffer (pH 6.8) comprising 250 µL of 0.06 M Tris-HCl with 100 µL of 10% concentrated glycerol. After centrifugation at 10,000×g for 20 min, the supernatant was collected. A control solution was prepared by combining 250 µL of 1 M Tris-HCl, 100 µL of 4 mM NAD^+, and 600 µL of distilled water, followed by adjustment to pH 8.8. A sample solution was prepared by mixing 250 µL of 1 M Tris-HCl (pH 8.8), 100 µL of 4 mM NAD^+, 100 µL of 1 M 95% ethanol, and 500 µL of distilled water, ensuring a homogeneous solution. For the assay, 950 µL of the control solution was added to cuvette 1 as the blank. Cuvette 1 contained 950 µL control (blank); cuvette 2 had 950 µL sample solution and 50 µL enzyme extract. After 5 min incubation, the absorbance at 340 nm was recorded. NADH concentration was calculated against a standard curve. Activity was expressed as µg NADH·mg^{-1} protein.

$$\text{ADH activity} = \frac{\text{NADH content}}{\text{Mw of NADH} \times \text{protein content}}$$

when Mw of NADH = 709.4 g.mol^{-1}

2.5.4 *Alcohol acetyltransferase (AAT) activity*

Extraction of AAT enzyme was adapted from Noichinda *et al*. [15]. Durian pulp (25 g) was ground at 4 °C and mixed with 33 mL of 0.2 M phosphate buffer (pH 7.0) containing 0.8 g of macerozyme, 1 g of polyvinyl polypyrrolidone (PVPP), and 0.1% Tween 20. The precipitate was washed with 8 mL of phosphate buffer (pH 8) twice and centrifuged at 23,000×g for 15 min. The supernatant was isolated for enzyme activity analysis, as referred to Aschariyaphotha *et al*. [5]. Enzyme extract (0.15 mL) was added to 0.85 mL of 0.5 M potassium phosphate buffer (pH 8.0), 100 µL of 11.6 mM $MgCl_2$, 20 µL of 0.3 mM acetyl-CoA, and 20 µL of 10 mM 99.8% methyl alcohol, combined thoroughly and allowed to rest for 15 min. After incubation, 50 µL of 10 mM 5,5′- dithiobis (2-nitrobenzoic acid) (DTNB) was added and incubated for 5 min. The absorbance was measured at 412 nm. DTNB forms a yellow complex with free CoA-SH. CoA-SH was quantified using a standard curve. Activity was expressed as µg CoA-SH·mg^{-1} protein.

$$\text{AAT activity} = \frac{\text{CoA} - \text{SH content}}{\text{Mw of CoA} - \text{SH} \times \text{protein content}}$$

when Mw of CoA-SH = 767.53 g·mol^{-1}

2.6 *Statistical analysis*

The experiment was designed as a Completely Randomized Design (CRD) with three replications. Data were analyzed using ANOVA, and mean differences were evaluated using Duncan's New Multiple Range Test (DMRT) at a 95% confidence level (p-value < 0.05). Multivariate analysis, including Principal Component Analysis (PCA) and a heatmap

of Pearson correlations, was performed using MetaboAnalyst 5.0 [26] to visualize differences in volatile profiles among the ripening stages. The PCA model was validated with a Permutational Multivariate Analysis of Variance (PERMANOVA) [27].

3 Results and Discussion

3.1 *Physiological dynamics related to fruit attributes of Monthong*

The respiratory behavior of Monthong durian during ripening exhibited a biphasic, or dual-climacteric, respiratory pattern. On the initial day, mature green fruit exhibited a respiration rate of 50 mg $CO_2 \cdot kg^{-1} \cdot h^{-1}$, which increased markedly to 180 mg $CO_2 \cdot kg^{-1} \cdot h^{-1}$ by day 4. The rate declined to 80 mg $CO_2 \cdot kg^{-1} \cdot h^{-1}$ on day 6, rose again to 160 mg $CO_2 \cdot kg^{-1} \cdot h^{-1}$ on day 7, and subsequently decreased gradually (Figure 1). This dual-climacteric peak (CP) behavior, consistent with Tongdee *et al*. [28], differentiates durian from other climacteric fruits. Mature green durians began to exhibit a climacteric rise two days after incubation at room temperature, with the first peak of climacteric respiration (CP1) occurring on day 4. This stage is marked by the separation of the pulp from the peel. Following a transient decline, the second peak (CP2) appeared on day 7, associated with pulp yellowing and mild aroma release. The husk, as a developing pericarp, performed higher respiration than the pulp [29]. Allowing the fruit to ripen beyond its optimal maturity stage resulted in progressive softening and intensified aroma. Dehiscence of the blossom end, indicative of the overripe stage [30], was observed on day 10.

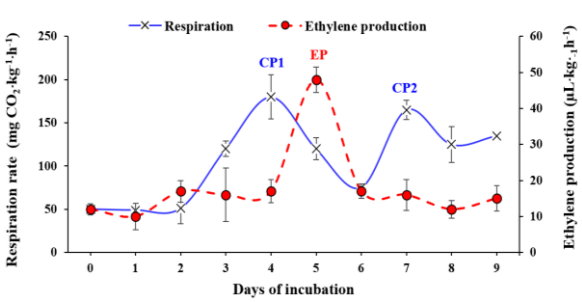

Figure 1: Respiration and ethylene production rates of Monthong durian fruit harvested at 80% maturity and incubated at 25 °C and 65–70% RH. Climacteric peak (CP), Ethylene production peak (EP).

Ethylene production of Monthong durian ranged from 10 to 15 μL $C_2H_4 \cdot kg^{-1} \cdot h^{-1}$ from day 1 to day 4, peaking at 48 μL $C_2H_4 \cdot kg^{-1} \cdot h^{-1}$ on day 5 before declining (Figure 1). This peak followed the first climacteric respiration peak by one day and aligned with CP2. During this stage, pericarp separation from the pulp was evident, with noticeable pulp yellowing (Figure S1 and Figure 2) and pulp softening (Figure 3), suggesting ethylene involvement in pericarp ripening and dehiscence [31].

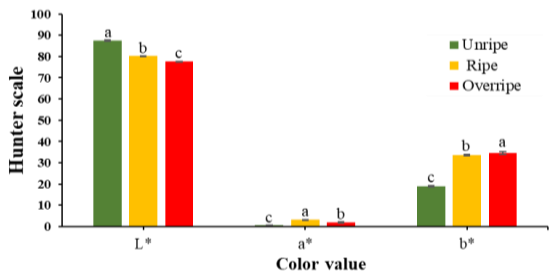

Figure 2: Changes in colors (L*, a*, and b*) of Monthong durian pulp during fruit maturation.

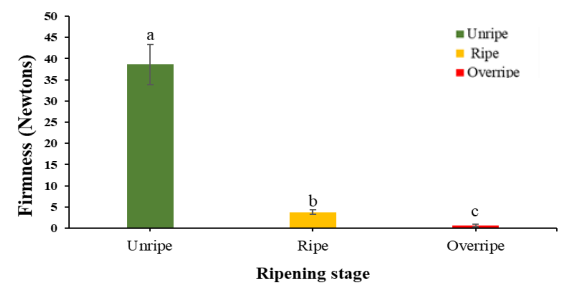

Figure 3: Changes in pulp firmness of Monthong durian fruit during maturation.

Monthong durians are oblong, thorn-covered fruits containing 4–5 segments. Pulp is developed from the seed funiculus, and husk from the ovary wall. Long pedicels and peduncles with defined abscission layers serve as ripening indicators. Fruit reaches full ripeness within 7 days postharvest. Biphasic respiration includes CP1, which corresponds to peduncle detachment and is unsuitable for consumption, followed by CP2 when husk color shifts, pulp softens, and aroma intensifies. Durian exhibits low ethylene production during the pre-climacteric stage, with a slight increase during the climacteric rise. Ethylene levels remain low during pre-climacteric stages, peak one day after CP1, and derive mainly from the husk, with minimal pulp contribution. Boonthanakorn *et al*., [32] noted that fresh-cut pulp

fails to ripen further due to limited ethylene biosynthesis, underscoring the husk's role in mediating ripening and aroma volatile synthesis. This dual-climacteric pattern provides critical insight into durian ripening physiology. Understanding the respiratory and ethylene production interplay offers a foundation for improving postharvest strategies to preserve fruit quality and extend shelf life.

3.2 *Evolution of volatile aroma compounds*

Aroma development in Monthong durian begins at ripening onset, initially marked by ethyl acetate and ethyl propanoate. As ripening progresses, ethyl butanoate production increases markedly (Table 1). Odor activity value (OAV) analysis identifies ethyl-2-methylpropanoate and ethyl butanoate as dominant odor-active compounds, contributing to the sweet, fruity, apple-like aroma of ripe durian. Additional esters, ethyl acetate, ethyl propanoate, and ethyl hexanoate, enhance the profile with fruit rum-like notes. Although methyl propanoate and propyl propanoate exhibit low OAVs, their non-ethanol origins contribute subtle rum-like nuances (Table 2). Compounds with OAVs >1.0 are considered key aroma contributors [33].

Table 1: Volatile compound content in Monthong durian pulp during 3 stages of fruit ripening.

Compound	RI	Volatile Content (ng thiophene·g^{-1} FW)		
		Unripe	Ripe	Overripe
Alcohol				
Ethanol	707	0.00	68.87	66.52
Aldehyde				
Acetaldehyde	703	0.00	26.34	14.42
Ester				
Methyl acetate	716	0.00	0.51	0.78
Ethyl acetate	733	0.00	28.95	24.87
Methyl propanoate	739	0.00	0.39	0.78
Ethyl propanoate	777	0.00	17.60	17.50
Ethyl-2-methyl propanoate	811	0.00	0.65	0.84
Methyl-2-methyl butanoate	827	0.00	0.00	0.17
Ethyl butanoate	849	0.00	0.55	1.35
Propyl propanoate	858	0.00	0.31	0.56
Ethyl (*E*)-2 butenoate	899	0.00	0.00	0.20
Ethyl-2-methyl butanoate	905	0.00	0.85	4.02
Ethyl hexanoate	1122	0.00	0.15	0.49
Terpenoid				
D-Limonene	1175	0.00	0.45	0.00
Sulfur compound				
Ethanethiol	713	0.00	10.59	8.01
Hexathiane	1500	3.93	0.00	0.00
Cyclic octaatomic sulfur	2049	2.12	0.00	0.00

RI - Retention Index

A heatmap (Figure 4) illustrates Pearson correlations among volatiles across three ripening stages. All esters are ripening-specific, with methyl-2-methylbutanoate and ethyl (E)-2-methylbutenoate exclusive to overripe pulp. Among sulfur volatiles, cyclic octaatomic sulfur and hexathiane appear in unripe pulp, while ethanethiol dominates in overripe fruit. D-limonene, present during early ripening, imparts fresh citrus-like. Strong positive correlations among ethyl hexanoate, ethyl butanoate, methyl acetate, and ethyl-2-methylbutanoate suggest coordinated accumulation, reinforcing the fruity-sweet aroma of ripe and overripe durian. Despite its low OAV, methyl-2-methylbutanoate may still enhance the sweet ester note.

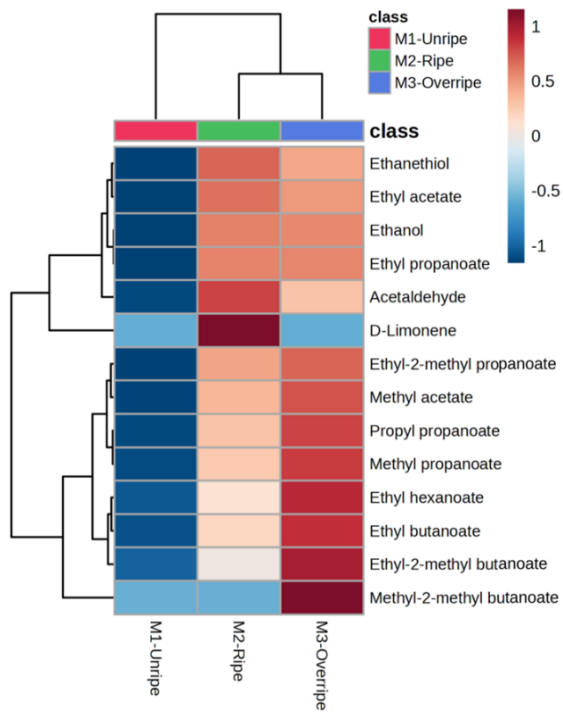

Figure 4: Correlation heatmap and dendrogram of volatile aroma compounds detected in Monthong durian across ripening stages.

Beyond esters, aldehydes and alcohols significantly influence aroma development. Both classes of compounds exhibit notable OAVs, with acetaldehyde being particularly influential due to its association with fermented and putrid odor characteristics. Furthermore, sulfur-containing compounds contribute substantially to durian's pungency. Ethanethiol, dominant in ripe fruit, has exceptionally high OAVs, imparting garlic-, onion-, and leek-like aromas. This is consistent with Li *et al*., [12] who reported ethanethiol in Monthong durian via solvent extraction. Synergistic interactions between sulfur volatiles and esters intensify durian's characteristic sharp odor. Volatile biosynthesis follows climacteric respiration, with CP1 marking ripening onset and CP2 coinciding with pericarp ripening and pulp softening. Hexathiane, detected solely in the mature green stage, may define early sulfur profiles. D-limonene, synthesized via *de novo* monoterpene biosynthesis, contributes citrus notes during early ripening but disappears at overripening (Table 1). These temporal changes offer valuable aroma-based markers for ripening stage differentiation.

Comprehensive profiling of esters, aldehydes, alcohols, sulfur volatiles, and terpenes facilitates postharvest strategies to optimize quality and extend shelf life. Ethyl-2-methylpropanoate (fruity), ethyl-2-methylbutanoate, ethyl propanoate (apple-like), ethyl butanoate (pineapple-like), ethyl acetate (rum-like), and ethyl hexanoate (green apple-like) shape the core odor profile. As ripening advances, ethanethiol becomes a major contributor to pungency due to its high OAV and sulfurous character. Ethionine, a precursor to ethanethiol [34], may be derived from cysteine alongside the biosynthesis of methionine [35]. Although sulfur compounds may evade direct olfactory detection, their synergistic effects are central to durian's distinctive pungency. Additionally, D-limonene (OAV = 11.9, Table 2), a monoterpene, found exclusively during early ripening and in durian peduncle sap (unpublished data), imparts citrus freshness valued by Thai consumers. Its absence in ripe fruit coincides with the emergence of pungent and rancid odors.

Principal component analysis (PCA) reveals distinct stage-specific clustering (Figure S2). PC1 (85.1%) and PC2 (14.9%) explain 99.9% of total variance. Unripe (M1: green circles) samples cluster on the positive PC1 axis, ripe (M2: red circles) on the negative PC1 and lower PC2, and overripe (M3: blue circles) on negative PC1 with elevated PC2 scores. The tight clustering of replicates within each stage and distinct separation between groups indicate consistent and stage-specific aroma profiles during durian ripening. The strong contribution of PC1 suggests that PC1 discriminates between unripe and ripe stages, while PC2 further separates ripe from overripe samples. PERMANOVA (Permutational Multivariate Analysis of Variance) confirms significant differences across stages ($F = 27{,}582$; $R^2 = 0.99978$; p-value = 0.001, 999 permutations), validating PCA as an effective tool for maturity discrimination based on volatile markers.

Table 2: Odor description, odor threshold, and odor active values of volatile compounds detected in overripe Monthong durian pulp.

Compounds	Volatile content*	Odor description	Odor threshold**†	OAV
Alcohol				
Ethanol	66.52	Solvent	0.62	107.29
Ethanethiol	8.01	Earthy, garlic, onion, sulfurous	0.000087	92,044.10
Aldehyde				
Acetaldehyde	14.42	Pungent, bruised apple	0.0015	9,615.00
Ester				
Methyl acetate	0.78	Sweet fruity	5.1	0.15
Ethyl acetate	24.87	Fruity, sweet, rum-like	0.88	28.27
Methyl propanoate	0.78	Fresh harsh fruity, strawberry, apple	0.35	2.24
Ethyl propanoate	17.50	Green, fruity, apple-like	1.1	15.91
Ethyl-2-methyl propanoate	0.84	Fruity	0.00011	7,651.22
Methyl-2-methyl butanoate	0.17	Sweet, fruity, apple-like	1.18	0.14
Ethyl butanoate	1.35	Fruity, pineapple	0.0036	374.01
Propyl propanoate	0.56	Pungent, sweet, fruity	0.28	2.00
Ethyl-(*E*)-2-butenoate	0.20	Fruity	n/a	n/a
Ethyl-2-methyl butanoate	4.02	Sweetly fruity, apple-like	0.00006	67,023.77
Ethyl hexanoate	0.49	Apple-like, fruity, sweet	0.01	48.78
Terpenoid				
D-Limonene	0.45	Fresh citrus-like	0.038	11.93

* ng thiophene·g^{-1} FW; ** values in air (μg·L^{-1})
† cited in van Gemert [36].

3.3 *Changes in amino acid, fatty acid and carboxylic precursors*

Monthong durian pulp contains high levels of amino acids, including aspartate, glutamate, alanine, cysteine, leucine, and proline with each exceeding 100 mg·100 g^{-1} FW. Many amino acids play pivotal roles in biochemical transformations during ripening, including the biosynthesis of aroma volatiles via

amino acid metabolism [37]. Aspartate, alanine, and valine increased significantly in the advanced ripening stage (Table 3). Meanwhile, isoleucine and leucine increased predominantly in the overripe stage, potentially contributing to late-stage physiological and aroma development. Methionine levels rose throughout ripening, though without statistically significant variation across stages.

Table 3: Amino acid contents detected in Monthong durian pulp during ripening stages.

Compound	Amino acid content (mg·100g^{-1} FW)*		
	Unripe	Ripe	Overripe
Aspartic acid (Asp)	255.58±2.10^{c}	311.07±1.95^{b}	367.38±1.88^{a}
Glutamic acid (Glu)	420.68±1.98^{a}	307.30±2.17^{c}	335.77±1.61^{b}
Serine (Ser) ^{ns}	65.77±1.25	65.97±2.49	64.99±1.07
Histidine (His)	24.57±1.56^{b}	31.63±1.61^{a}	28.68±1.41^{a}
Glycine (Gly)	69.26±1.25^{b}	78.54±2.48^{a}	74.96±1.87^{a}
Threonine (Thr)	56.51±0.17^{a}	52.60±0.89^{c}	54.12±0.91^{b}
Arginine (Arg)	61.86±0.07^{a}	55.85±1.17^{b}	61.07±0.14^{a}
Alanine (Ala)	116.47±2.93^{c}	223.39±2.68^{b}	302.29±2.75^{a}
Tyrosine (Tyr)	36.46±0.06^{b}	30.88±1.14^{c}	37.90±0.13^{a}
Cysteine (Cys)	138.80±2.02^{a}	130.77±2.20^{b}	124.70±2.81^{c}
Valine (Val)	67.96±1.07^{c}	70.29±1.03^{b}	80.74±1.06^{a}
Methionine (Met)	12.45±0.97^{b}	16.29±1.04^{a}	16.12±1.06^{a}
Phenylalanine (Phe)	59.33±0.05^{c}	61.24±0.28^{b}	67.17±0.85^{a}
Isoleucine (Ile)	54.16±0.03^{b}	54.49±0.70^{b}	60.61±0.65^{a}
Tryptophan (Trp)	6.01±0.05^{c}	11.88±0.97^{a}	8.73±0.03^{b}
Leucine (Leu)	99.15±0.06^{b}	100.02±1.01^{b}	106.83±1.63^{a}
Lysine (Lys)	85.81±1.55^{c}	93.20±0.82^{b}	97.72±0.96^{a}
Proline (Pro)	101.96±2.03^{b}	98.74±1.28^{b}	106.12±1.99^{a}

*Data are expressed as means ± SD (n = 3). Values in the same row followed by different letters indicate significant differences at p-value < 0.05 according to Duncan's multiple range test.

The findings strongly support the hypothesis that amino acids are precursors to volatile substances such as durian's branched-chain esters and sulfurous volatiles. Branched-chain amino acids (BCAAs), including leucine, isoleucine, and valine, increase throughout ripening and peak when the fruit is overripe. Fruity flavors come from their branched-chain esters, which emerged and rose with this trend [38]. The increase in isoleucine corresponds with the notable rise of ethyl-2-methyl butanoate, a key durian ester (Table 1). Regarding threonine metabolism, it is plausible to ethanol formation, as it is convertible into acetaldehyde, an intermediate reducible to ethanol [39]. However, the specific role of threonine-derived acetaldehyde in durian ethanol biosynthesis warrants further investigation. Declining cysteine and rising methionine levels support their roles in ethylene biosynthesis (Figure 1) and sulfur volatile production [8]. Methionine has its peak at the ripe stage (16.29 mg·100g^{-1} FW), matching a rise in ethanethiol (10.59 ng·g^{-1} FW). Notably, alanine concentrations double from unripe to overripe. Alanine could convert to pyruvate, a key metabolite and acetyl-CoA precursor under hypoxic conditions [40], as found in durian fruit. The alcohol moiety in many esters, ethanol, is produced from acetyl-CoA, a precursor to the acyl component. The high alanine level suggests that it is the main substrate for the substantial production of esters such as ethyl esters and acetate esters during ripening. Furthermore, glutamic acid, the most prevalent amino acid in unripe durian, exhibits a decline in concentration as the fruit ripens. This suggests that it may serve as a carbon skeleton provider for the intensive metabolic processes [41] involved in volatile synthesis. Persistently high levels of aspartate, glutamate, and alanine throughout maturation suggest broad metabolic functionality.

Total lipid content was significantly higher in ripe pulp compared to unripe fruit (Figure 5(a)), indicating lipid accumulation during ripening. Palmitic acid ($C_{16:0}$) and oleic acid ($C_{18:1}$) were the predominant components, consistently exhibiting the highest concentrations across all stages of maturation (Figure 5(b)). These contribute to membrane structure and may influence texture and sensory attributes. In contrast, linoleic acid ($C_{18:2}$) declined progressively during the ripening process, whereas linolenic acid ($C_{18:3}$) increased during early ripening and decreased thereafter. These shifts suggest conversion of polyunsaturated fatty acids (PUFAs) into aroma-related volatiles, a process common in climacteric fruits [42]. This transition aligns with increased lipoxygenase (LOX) activity during ripening (Figure 6(a)), similar to the LOX response to ethylene, which produces volatiles in tomato fruit [43]. LOX likely facilitates the formation of aldehydes and alcohols via its pathway, contributing to durian's characteristic aroma. These metabolic changes underscore the complex biochemical interactions governing lipid modification and volatile synthesis during ripening.

Four short-chain carboxylic acids, acetic (C_2), propanoic (C_3), butanoic (C_4), and hexanoic acid (C_6), were detected in durian pulp. Acetic acid increased sharply from 8.95 to 201.51 mg·100 g^{-1} FW from ripe to overripe stages (Table 4). Notably, propanoic acid

was present throughout fruit maturation from 1.59 mg·100 g^{-1} FW in unripe pulp and increased 5-fold in ripe to 20-fold at overripe stages. On the other hand, butanoic and hexanoic acids were found in small amounts (<1 mg·100 g^{-1} FW) in ripe and overripe stages. Acetyl-CoA production significantly increases during ripening, primarily via β-oxidation as seen in papaya ripening [44] and partially through fermentation, where acetaldehyde is converted into acetate, then acetyl-CoA [45]. The progressive accumulation of C_3 acids may originate from fatty acid biosynthesis, beginning with succinic acid or succinyl-CoA from the Krebs cycle and proceeding via α-oxidation to form propionic acid [46], whereas C_4 acids from β-oxidation; and C_6 from LOX-mediated degradation [16]. These acids are converted into acyl-CoA by ACS [47], providing substrates for ester biosynthesis. Ester biosynthesis, the dominant contributor to durian aroma, is catalyzed by alcohol acyltransferase (AAT) [48], which utilizes alcohols and carboxylic acids arising from lipid, protein, and carbohydrate degradation.

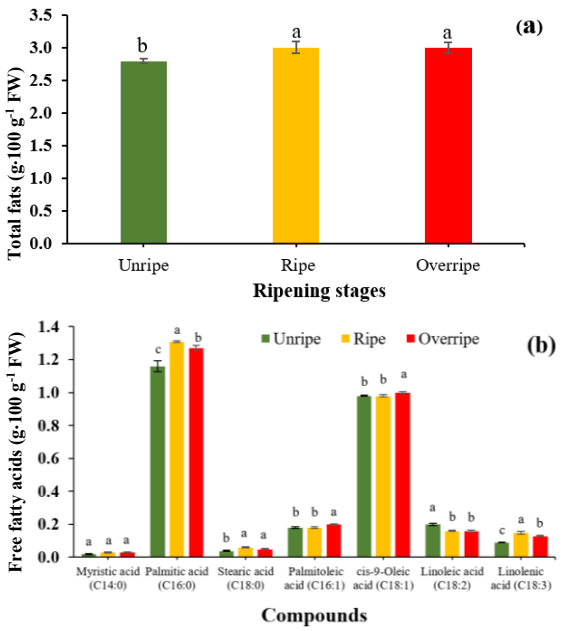

Figure 5: Total fats (a) and free fatty acids (b) in Monthong durian pulp of fruit during unripe, ripe and overripe stages.

Table 4: Carboxylic acid contents detected in Monthong durian pulp during ripening stages.

Compounds	Short Chain Fatty Acid Content (mg·100 g^{-1} FW)*		
	Unripe	Ripe	Overripe
Acetic acid (C_2)	nd	8.95 ± 0.60^{bA}	201.51 ± 6.69^{aA}
Propanoic acid (C_3)	1.59 ± 0.09^{c}	7.87 ± 0.10^{bB}	33.37 ± 0.27^{aB}
Butanoic acid (C_4)	nd	0.19 ± 0.00^{bC}	0.46 ± 0.04^{aC}
Hexanoic acid (C_6)	nd	0.14 ± 0.01^{bC}	0.58 ± 0.12^{aC}

* Data are expressed as means ± SD (n = 3). Values in the same row followed by different small letters and in the same column followed by different capital letters indicate significant differences at $P<0.05$ according to Duncan's multiple range test. nd = not detected.

3.4 *Role of enzymes in volatile formation*

LOX activity remained high throughout ripening and increased sharply by approximately one-third in the overripe stage (Figure 6(a)). In durian pulp, many volatile ester precursors originate from lipid-derived oxidation pathways, including β-oxidation and LOX, which generate short-chain aldehydes and alcohols. Alcohol dehydrogenase (ADH), which catalyzes aldehyde-to-alcohol conversion, showed a progressive increase from unripe to overripe stages (Figure 6(b)), reflecting its central function in volatile formation. ADH also reversibly converts alcohols back to aldehydes, enabling dynamic flux between intermediates. Aldehyde dehydrogenase (ALDH), responsible for oxidizing aldehydes into carboxylic acids, increased steadily during maturation (Figure 6(c)), consistent with patterns observed in banana ripening [49]. The concurrent rise in short-chain carboxylic acids (Table 4) supports ALDH's role in regulating volatile precursors. These acids are subsequently activated by acyl-CoA synthase (ACS), forming substrates essential for ester biosynthesis. Alcohol acetyltransferase (AAT) activity was negligible in unripe durian pulp (Figure 6(d)), explaining the absence of detectable esters at this stage. Ethylene production was minimal during early development (10–15 $\mu L \cdot kg^{-1} \cdot h^{-1}$) but tripled to 48 $\mu L \cdot kg^{-1} \cdot h^{-1}$ in ripe fruit (Figure 1), coinciding with enhanced ester biosynthesis (Tables 1 and 2). Limited ester formation in unripe pulp may result from substrate scarcity, particularly alcohols and carboxylic acids. AAT activity increased markedly in ripe pulp and peaked in the overripe stage, reinforcing its essential role in aroma development. In Xiaobai apricot, LOX and AAT activities were positively correlated with ester variation during postharvest storage [50].

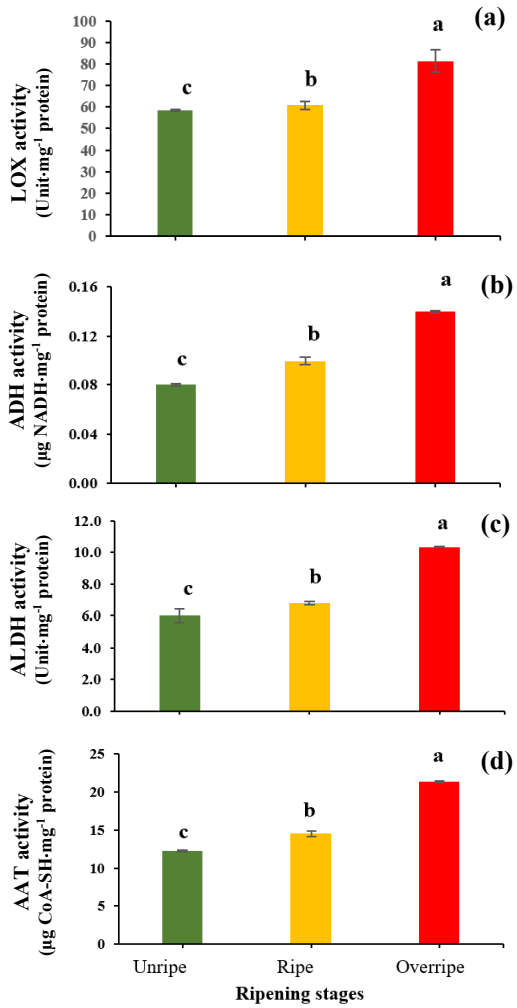

Figure 6: Activities of lipoxygenase (LOX) (a), alcohol dehydrogenase (ADH) (b), Aldehyde dehydrogenase (ALDH) (c), and alcohol acetyltransferase (AAT) (d) in Monthong durian pulp of fruit during unripe, ripe, and overripe stages.

These findings highlight a strong link between respiration and ester biosynthesis, influenced by various external and internal factors. Controlled or modified atmosphere conditions [51], low-temperature storage [52], and minimal processing [53] influence ripening and ester production by altering respiratory metabolism. Ethylene, the primary regulator of ester biosynthesis, modulates AAT expression in an ethylene-dependent manner. Nevertheless, some fruits contain high alcohol concentrations and exhibit AAT activity; their corresponding esters are not always detectable. For instance, tomatoes contain significant methyl alcohols but lack methyl esters, while certain non-climacteric fruits (e.g., strawberries [54], and pineapple [55]) produce volatile esters despite low ethylene levels, indicating that even minimal ethylene can trigger ester biosynthesis. Interestingly, AAT activity was detected in mature green durian pulp, yet no ester production occurred despite high concentrations of alcohols and acids such as ethanol and propanoic acid. This may suggest that propanoic acid is not converted into propionyl-CoA, the required precursor for ester formation. Further characterization of ethylene-dependent ester biosynthesis revealed distinct temporal patterns, with EP occurring after CP1 but before CP2, when ethylene enhances AAT activity and initiates ester accumulation.

3.5 *Integrated view of aroma biosynthesis in durian*

3.5.1 Dynamic changes in ester volatiles during fruit ripening

Esters were undetectable in unripe durian pulp but began accumulating during ripening. Straight-chain esters, including methyl acetate, ethyl acetate, methyl propanoate, ethyl propanoate, ethyl butanoate, and ethyl hexanoate, were synthesized during this phase. In the overripe stage, only ethyl butanoate and ethyl hexanoate showed modest increases (Figure 7(a)), indicating continued formation into full maturity. Branched-chain esters, absent in unripe pulp, emerged during ripening, particularly ethyl-2-methylbutanoate and ethyl-2-methylpropanoate (Figure 7(b)). Ethyl-2-methylbutanoate, identified as a key aroma compound in ripe durian, increased threefold in overripe samples compared to ripe fruit, enhancing durian's characteristic scent. Straight-chain esters are likely synthesized via fatty acid β-oxidation, a pathway upregulated during papaya ripening [44], suggesting conservation across tropical climacteric fruits. In ripe durian pulp, ethyl esters dominated the profile (63.6%), followed by methyl (27.3%) and propyl esters (9.1%) (Figure S3(a)). These were further classified into short-chain (72.7%) and branched-chain esters (27.3%) (Figure S3b), emphasizing the central role of short-chain esters in aroma development. The progressive emergence of branched esters contributes to the complexity and richness of durian flavor.

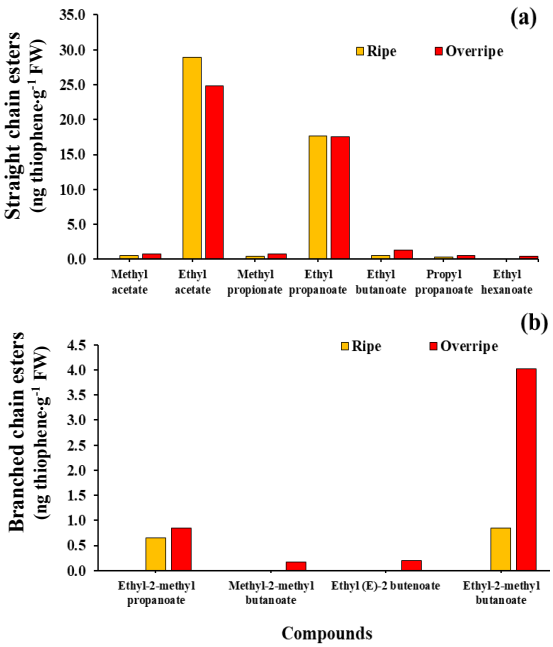

Figure 7: Amounts of straight chain esters (a) and branched chain esters (b) in Monthong durian pulp during ripe and overripe stages.

3.5.2 Consequences of volatile esters produced during durian ripening

Durian's distinctive odor intensifies as ripening progresses, driven by ester production. Ripe pulp exhibits elevated ethanol and acetaldehyde levels, suggesting enhanced respiration and localized hypoxia due to the thick husk, which promotes anaerobic metabolism. This shift accelerates ethanol and acetaldehyde accumulation, contributing to the fermented aroma of late-stage durian. Early ripening favors the synthesis of short-chain esters such as ethyl acetate and ethyl propanoate, derived from fatty acid metabolism. As ripening advances, esters including ethyl-2-methylpropanoate, ethyl butanoate, ethyl-2-methylbutanoate, and ethyl hexanoate intensify. Overripening enhances amino acid-derived esters, particularly ethyl-2-methylbutanoate and methyl-2-methylbutanoate. Ethyl-2-methylpropanoate originates from valine, while methyl-2-methylbutanoate and ethyl-2-methylbutanoate derive from isoleucine metabolism [38]. Based on their OAVs, durian esters can be classified into three distinct categories. Initially, the presence of thyl-2-methylpropanoate and ethyl-2-methylbutanoate within high OAV significantly shapes the aroma profile. Furthermore, moderate OAV encompasses ethyl butanoate, which significantly enhances the distinctive aroma. Finally, low OAV includes ethyl acetate, ethyl hexanoate, and ethyl propanoate, which provide subtle odor enhancements. This classification underscores dynamic shifts in ester composition and their essential role in defining durian's odor profile.

3.5.2 Substrates supporting volatile ester biosynthesis

Fatty acid contents underscore their importance as reservoirs for acyl groups used in ester formation. Beta-oxidation of fatty acids during ripening yields acetyl-CoA and short-chain acyl CoA [51]. The predominant fatty acids in durian pulp are palmitic acid ($C_{16:0}$) and cis-9-oleic acid ($C_{18:1}$), whose high and stable concentrations suggest a substantial precursor pool. The LOX pathway contributes to the diversity of the volatile profile by generating precursors from fatty acids. LOX activity dramatically increased in the ripe stages (Figure 6(a)), acting on PUFAs like linoleic acid ($C_{18:2}$) and linolenic acid ($C_{18:3}$) (Figure 5(b)) to produce hydroperoxides. These intermediates are subsequently converted into a range of aldehydes and alcohols. Linoleic acid ($C_{18:2}$) declined from the unripe to ripe stage and may be oxidized into C_6 molecules [16], serving as substrates for ethyl hexanoate during ripening (Table 1), contributing to the complexity of durian aroma. Linolenic acid ($C_{18:3}$) rose from the unripe to the ripe stage, followed by a slight decline. This fatty acid is a precursor for jasmonates and other signaling molecules that govern fruit ripening [56] and scent, suggesting indirect modulation.

The production of straight-chain esters, which peaks in the ripe stage, and the accumulation of acetic acid in the overripe stage are directly controlled by the competing activities of ADH and ALDH. ADH activity increased in the ripe stages (Figure 6(b)), facilitating the reduction of aldehydes into their corresponding alcohols. This is evident from the large amount of ethanol (68.87 ng·g^{-1} FW) detected in the ripe pulp (Table 1), which serves as the primary alcohol substrate for AAT, leading to a peak in ethyl ester production. A significant metabolic shift occurs in the overripe stage, while ALDH activity surges to its maximum level (Figure 6(c)). This redirects acetaldehyde away from alcohol formation toward oxidation, resulting in a dramatic increase in acetic acid from 8.95 mg·100g^{-1} FW in the ripe stage to 201.51 mg·100g-1 FW in the overripe stage (Table 4).

This indicated that the elevated ALDH activity is directly responsible for the significant accumulation of acetic acid in overripe fruit.

Branched-chain amino acids (BCAAs)—valine, leucine, and isoleucine (Figure 8)—steadily increase and reach their highest concentrations in the overripe stage (Table 3). These amino acids serve as precursors for branched-chain alcohols and acids required for ester synthesis [38]. Crucially, AAT activity spikes dramatically in the overripe stage, surpassing levels observed in the ripe stage (Figure 6(d)). The convergence of elevated BCAA precursors and heightened AAT activity creates optimal conditions for ester biosynthesis, directly causing the sharp increase in branched-chain esters observed in the overripe stage (Figure 7(b)). Consequently, dynamic changes in amino acids undergo metabolic transformations, yielding volatiles and secondary metabolites. Some may be stored as glutathione and mobilized during ripening, as reported by Panpetch and Sirikantaramas [57] in the context of sulfur metabolism. Acetyl-CoA, abundantly produced in ripe durian, may also be metabolized into propanoic acid via acetyl-CoA carboxylase, forming succinyl-CoA through alternative routes (Figure 8). Branched-chain esters reflect tight biochemical integration between amino acid turnover and ester synthesis, key to durian's aroma complexity.

In summary, in the ripe stage, elevated activities of ADH and LOX enhance the production of alcohols and other precursors, which, in conjunction with active AAT, result in a peak in the synthesis of straight-chain esters. A metabolic switch takes place during the overripe stage. An increase in ALDH activity directs aldehyde precursors towards significant acetic acid buildup. At the same time, a significant increase in AAT activity, along with a higher availability of BCAAs, drives the rapid synthesis of the desirable branched-chain esters. This shows that the activities of ADH, ALDH, and AAT are key regulatory points that, by acting on available substrate pools, directly shape the distinct aroma profiles of ripe and overripe durian fruit.

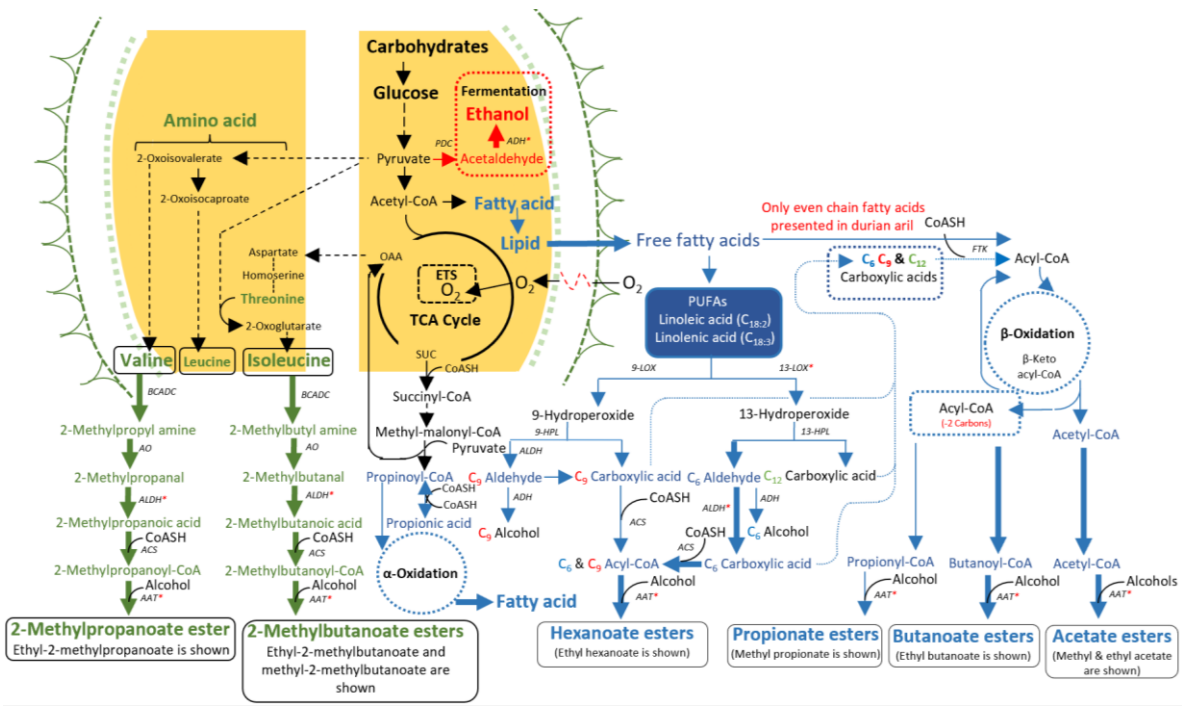

Figure 8: Putative biosynthetic pathways of volatile esters conducted in ripe durian pulp.

4 Conclusions

The ripening of Monthong durian is a complex, ethylene-regulated process defined by biphasic respiration. After CP1, elevated ethylene levels started CP2 and biosynthesized and released ester and sulfur-containing volatiles. According to OAVs, ethanethiol, ethyl-2-methyl butanoate, ethyl-2-methyl propanoate, ethyl butanoate, and ethyl hexanoate, together with fermented notes from ethanol and acetaldehyde, dominated durian's aroma. Mostly alcohol-derived volatile esters were ethyl (63.6%), methyl (27.3%), and propyl (9.1%). Straight-chain (72.7%) and branched-chain (27.3%) esters exist. During the fruit ripening process, straight-chain esters, derived primarily from fatty acid metabolism, define the aroma of ripe fruit, while branched-chain esters, synthesized from amino acid precursors, become prominent in the overripe stage. The accumulation of branched-chain amino acids (valine, leucine, and isoleucine) and the concurrent spike in alcohol acetyltransferase (AAT) activity in the overripe stage facilitate the production of branched-chain esters. Meanwhile, increased lipoxygenase (LOX) and aldehyde dehydrogenase (ALDH) activities modulate the pool of fatty acid-derived precursors. This comprehensive model of aroma biosynthesis in durian, highlights the coordinated regulation of amino acid and fatty acid metabolism. The distinct volatile profiles of each ripening stage, such as the exclusive presence of hexathiane in unripe fruit and the dominance of ethyl-2-methylbutanoate at peak ripeness, can serve as objective biomarkers for maturity and quality assessment. This knowledge creates opportunities for developing novel postharvest strategies, such as using targeted elicitors to modulate specific aroma profiles, thereby enhancing consumer preference and improving fruit quality management.

Acknowledgments

The authors express their deep appreciation to Rajamangala University of Technology Phra Nakhon for providing the partial funds for Ms. Duangkamol Tungsatitporn. Thanks are reserved for the Postharvest Technology Innovation Center, Office of the Ministry of Higher Education, Science, Research and Innovation, Thailand, and the Center for Agricultural Systems Biology and the United Graduate School of Agricultural Science (UGSAS), Gifu University, Japan, for providing us with the facilities.

Author Contributions

D.T.: data curation, methodology, formal analysis, writing-original draft; C.W.: writing-reviewing and editing, conceptualization, validation, supervision; B.I.M.: data curation, software; W.A.: resources, methodology, investigation; K.B.: validation, visualization; S.N.: project administration, writing–reviewing, investigation, supervision. All authors have read and agreed to the published version of the manuscript.

Conflicts of Interest

Duangkamol Tungsatitporn reports financial support was partially provided by Rajamangala University of Technology Phra Nakhon. If there are other authors, they declare that they have no known competing financial interests or personal relationships that could have appeared to influence the work reported in this paper.

References

[1] N. A. W. A. Ali, G. R. Wong, B. C. Tan, W. S. Lum, and P. Mazumdar, "Unleashing the potential of durian: Challenges, opportunities, and the way forward," *Applied Fruit Science*, vol. 67, 2025, Art. no. 3, doi: 10.1007/s10341-024-01237-y.

[2] P. Likhitpichitchai, J. Khermkhan, and S. Kuhaswonvetch, "The competitiveness of Thai durian export to China's market," *GMSARN International Journal*, vol. 17, pp. 371–378, 2023.

[3] Anonymous. "Demand for durian in the world market is set to surge 400%, Thailand benefits from the popularity of durian in Chaina." Infoquest.co.th. Accessed: Oct. 13, 2025. [Online.] Available: https://www.infoquest.co.th/2023/334785

[4] B. Jirawut et al., "Postharvest management of durian: The production system and management of quality durians throughout supply chains to chinese market," Department of Agriculture, Thailand, Ink-On Paper Co. Ltd., Bangkok, 2024.

[5] W. Aschariyaphotha, C. Wongs-Aree, K. Bodhipadma, and S. Noichinda, "Fruit volatile fingerprints characterized among four commercial cultivars of Thai durian (*Durio zibethinus*)," *Journal of Food Quality*, vol. 2021, 2021, Art. no. 1383927, doi: 10.1155/2021/1383927.

[6] E. Sospeter et al., "Understanding the complex aroma profile of durian fruit: A concise review," *Food Science*, vol. 90, 2024, Art. no. e70099, doi: 10.1111/1750-3841.70099.

[7] W. Phutdhawong, P. Chairat, K. Kantarod, and W. Phutdhawong, "GC-MS and 1 H NMR analysis of fatty acids in Monthong Thai durian (*Durio zibethinus* Murr)," *Chemical Science Transactions*, vol. 4, no. 3, pp. 663–667, 2015, doi: 10.7598/cst2015.1068.

[8] L. Sangpong et al., "Assessing dynamic changes of taste-related primary metabolism during ripening of durian pulp using metabolomic and transcriptomic analyses," *Frontiers in Plant Science*, vol. 12, Jun. 2021, Art. no. 687799, doi: 10.3389/fpls.2021.687799.

[9] A. Wisutiamonkul, S. Promdang, S. Ketsa, and W. G. van Doorn, "Carotenoids in durian growth and postharvest ripening," *Food Chemistry*, vol. 180, pp. 301–305, Aug. 2015, doi: 10.1016/j.foodchem.2015.01.129.

[10] G. Khaksar, S. Kasemcholathan, and S. Sirikantaramas, "Durian (*Durio zibethinus* L.): Nutritional composition, pharmacological implications, value-added products, and omics-based investigations," *Horticulturae*, vol. 10, no. 4, Mar. 2024, Art. no. 342, doi: 10.3390/horticulturae10040342.

[11] S. Mostafa, Y. Wang, W. Zeng, and B. Jin, "Floral scents and fruit aromas: Functions, compositions, biosynthesis, and regulation," *Frontiers in Plant Science*, vol. 13, Mar. 2022, Art. no. 860157, doi: 10.3389/fpls.2022.860157.

[12] J. -X. Li, P. Schieberle, and M. Steinhaus, "Characterization of the major odor-active compounds in Thai durian (*Durio zibethinus* L. 'Monthong') by aroma extract dilution analysis and headspace gas chromatography−olfactometry," *Agricultural and Food Chemistry*, vol. 60, no. 45, pp. 11253−11262, Oct. 2012, doi: 10.1021/jf303881k.

[13] F. Yang et al., "Changes and correlation analysis of volatile flavor compounds, amino acids, and soluble sugars in durian during different drying processes," *Food Chemistry: X*, vol. 21, Mar. 2024, Art. no. 101238, doi: 10.1016/j.fochx.2024.101238.

[14] C. Wongs-Aree and S. Noichinda, "Postharvest quality properties of potential tropical fruits related to their unique structural characters," in *Postharvest Handling: A Systems Approach (4th Editions)*, W. J. Florkowski, N. H. Banks, R. L. Shewfelt, and S. E. Prussia, Eds., Oxford, UK: Academic Press, 2022, pp. 277–316.

[15] S. Noichinda, Y. Ueda, Y. Imahori, and K. Chachin, "Thioester production and thioalcohol specificity of alcohol acetyltransferase in strawberry fruit," *Food Science and Technology*, vol. 5, no. 1, pp. 99–103, 1999, doi: 10.3136/fstr.5.99.

[16] W. Zhou, W. Kong, C. Yang, R. Feng, and W. Xi, "Alcohol acyltransferase is involved in the biosynthesis of C_6 esters in apricot (*Prunus armeniaca* L.) fruit," *Frontiers in Plant Science*, vol. 12, Nov. 2021, Art. no. 763139, doi: 10.3389/fpls.2021.763139.

[17] H. Zhao, D. K. Kosma, and S. Lu, "Functional role of long-chain acyl-CoA synthetases in plant development and stress responses," *Frontiers in Plant Science*, vol. 22, Mar. 2021, Art. no. 640996, doi: 10.3389/fpls.2021.640996.

[18] N. X. B. Nguyen, T. Saithong, P. Boonyaritthongchai, M. Buanong, S. Kalapanulak, and C. Wongs-Aree, "Methyl salicylate induces endogenous jasmonic acid and salicylic acid in 'Nam Dok Mai' mango to maintain postharvest ripening and quality," *Plant Physiology*, vol. 303, Dec. 2024, Art. no. 154356, doi: 10.1016/j.jplph.2024.154356.

[19] Z. Li, T. Hong, Z. Zhao, Y. Gu, Y. Guo, and J. Han, "Fatty acid profiles and nutritional evaluation of fresh sweet-waxy corn from three regions of China," *Foods*, vol. 11, no. 17, Aug. 2022, Art. no. 2636, doi: 10.3390/foods11172636.

[20] L. Lenti, A. Nartea, O. L. Orhotohwo, D. Pacetti, and D. Fiorini, "Development and validation of a new GC-FID method for the determination of short and medium chain free fatty acids in wine," *Molecules*, vol. 27, no. 23, Nov. 2022, Art. no. 8195, doi: 10.3390/molecules27238195.

[21] B. T. Amid, H. Mirhosseini, and S. Kostadinović, "Chemical composition and molecular structure of polysaccharide-protein biopolymer from *Durio zibethinus* seed: Extraction and purification process," *Chemistry Central Journal*, vol. 6, Oct. 2012, Art. no. 117, doi: 10.1186/1752-153X-6-117.

[22] M. M. Bradford, "A rapid and sensitive method for the quantitation of microgram quantities of protein utilizing the principle of protein-dye binding," *Analytical Biochemistry*, vol. 72, no. 1–2, pp. 248–254, May 1976, doi: 10.1006/abio.1976. 9999.

[23] L. Sirikesorn, W. Imsabai, S. Ketsa, and W.G. van Doorn, "Ethylene-induced water soaking in *Dendrobium* floral buds, accompanied by increased lipoxygenase and phospholipase D (PLD) activity and expression of a PLD gene," *Postharvest Biology and Technology*, vol. 108, pp. 48–53, Oct. 2015, doi: 10.1016/j.postharvbio. 2015.04.009.

[24] N. Meguro, H. Tsuji, Y. Suzuki, N. Tsutsumi, A. Hirai, and M. Nakazono, "Analysis of expression of genes for mitochondrial aldehyde dehydrogenase in maize during submergence and following reaeration," *Breeding Science*, vol. 56, no. 4, pp. 365–370, 2006, doi: 10.1270/jsbbs. 56.365.

[25] T. Okamura et al., "Characteristics of wine produced by mushroom fermentation," *Bioscience and Bioengineering*, vol. 65, no.7, pp. 1596–1600, May 2001, doi: 10.1271/ bbb.65.1596.

[26] Z.Pang, G. Zhou, J. Chong, X. Dong, and J. Xia, "MetaboAnalyst 5.0: narrowing the gap between raw spectra and functional insights," *Nucleic Acids Research*, vol. 49, no. W1, W388–W396, May 2021, doi: 10.1093/nar/gkab382.

[27] M. J. Anderson, *Permutational Multivariate Analysis of Variance (PERMANOVA)*. NJ: Wiley, Nov. 2017, pp. 1–15.

[28] S. C. Tongdee, A. Suwanagul, and S. Neamprem, "Durian fruit ripening and the effect of variety, maturity stage at harvest, and atmosphere gases," *Acta Horticulturae*, vol. 269, pp. 323–334, 1990, doi: 10.17660/ActaHortic.1990.269.43.

[29] P. Brooncherm and J. Siriphanich, "Postharvest physiology of durian pulp and husk," *Kasetsart Journal (Natural Science)*, vol. 25, no. 5, pp. 119–125, Dec. 1991.

[30] L. Khurnpoon and J. Siriphanich, "Changes in pectin fractions and enzyme activities during husk dehiscence of Monthong durians," *Acta Horticulturae*, vol. 687, pp. 187–192, 2005, doi: 10.17660/ActaHortic.2005.687.22.

[31] Y. Palapol, S. Kunyamee, M. Thongkhum, S. Ketsa, I. B. Ferguson, and W. G. van Doorn, "Expression of expansin genes in the pulp and the dehiscence zone of ripening durian (*Durio zibethinus*) fruit," *Plant Physiology*, vol. 182, pp. 33–39, Jun. 2015. doi: 10.1016/j.jplph.2015.04. 005.

[32] J. Boonthanakorn, W. Daud, A. Aontee, and C. Wongs-Aree, "Quality preservation of fresh-cut durian cv. 'Monthong' using microperforated PET/PE films," *Food Packaging and Shelf Life*, vol. 23, Mar. 2020, Art. no. 100452, doi: 10.1016/j.fpsl.2019.100452.

[33] A. Laura, V. Luciano, G. Josep, B. Olga, and M. Montserrat, "Chemical characterization of commercial sherry vinegar aroma by headspace solid-phase microextraction and gas chromatography-olfactometry," *Agricultural and Food Chemistry*, vol. 59, no. 8, pp. 4062–4070, Mar. 2011, doi: 10.1021/jf104763u.

[34] N. S. Fischer and M. Steinhaus, "Identification of an important odorant precursor in durian: First evidence of ethionine in plants," *Agricultural and Food Chemistry*, vol 68, no. 38, pp. 10397−10402, Dec. 2019, doi: 10.1021/acs.jafc. 9b07065.

[35] V. Gorelova, L. Ambach, F. Rebeille, C. Stove, and D. van Der Straeten, "Folates in plants: Research advances and progress in crop biofortification," *Frontiers in Chemistry*, vol. 5, Mar. 2017, Art. no. 21, doi: 10.3389/fchem. 2017.00021.

[36] L. J. van Gemert, *Odour Thresholds (revised edition)*. Utrecht, Netherlands: Oliemans Punter & Partners BV, 2011.

[37] I. Maoz, E. Lewinsohn, and I. Gonda, "Amino acids metabolism as a source for aroma volatiles biosynthesis," *Current Opinion in Plant Biology*, vol. 67, Jun. 2022, Art. no. 102221, doi: 10.1016/ j.pbi.2022.102221.

[38] P. Engelgau, S. K. Wendakoon, N. Sugimoto, and R. M. Beaudry, "Fruits produce branched-chain esters primarily from newly synthesized precursors," *Agricultural and Food Chemistry*, vol. 73, no. 7, pp. 4196–4207, Feb. 2025, doi: 10.1021/acs.jafc.4c10677.

[39] V. Joshi, J. G. Joung, Z. Fei, and G. Jander, "Interdependence of threonine, methionine and isoleucine metabolism in plants: Accumulation and transcriptional regulation under abiotic stress," *Amino Acids*, vol. 39, no. 4, pp. 933–947, Feb. 2010, doi: 10.1007/s00726-010-0505-7.

[40] L. T. Bui et al., "Conservation of ethanol fermentation and its regulation in land plants,"

Experimental Botany, vol. 70, no. 6, pp. 1815–1827, Feb. 2019. doi: 10.1093/jxb/erz052

[41] H.-S. Liao, Y.-H. Chung, and M.-H. Hsieh, "Glutamate: A multifunctional amino acid in plants," *Plant Science*, vol. 318, May 2022, Art. no. 111238, doi: 10.1016/j.plantsci.2022.111238.

[42] J. Song and F. Bangerth, "Fatty acids as precursors for aroma volatile biosynthesis in pre-climacteric and climacteric apple fruit," *Postharvest Biology and Technology*, vol. 30, no. 2, pp. 113−121, Nov. 2003, doi: 10.1016/S0925-5214(03) 00098-X.

[43] A. A. Velázquez-López et al., "Lipoxygenase and its relationship with ethylene during ripening of genetically modified tomato (*Solanum lycopersicum*)," *Food Technology and Biotechnology*, vol. 58, no. 2, pp. 223–229, Jun. 2020. doi: 10.17113/ftb.58.02.20.6207.

[44] R. G. der Agopian, J. P. Fabi, and B. R. Cordenunsi-Lysenko, "Metabolome and proteome of ethylene-treated papayas reveal different pathways to volatile compounds biosynthesis," *Food Research International*, vol. 131, May 2020, Art. no. 108975, doi: 10.1016/j.foodres.2019.108975.

[45] C. Wongs-Aree and S. Noichinda, "Glycolysis fermentative by-products and secondary metabolites involved in plant adaptation under hypoxia during pre- and postharvest (Chapter 4)," in *Hypoxia and Annoxia*, K. Das and M. S. Biradar, Eds., London, UK: IntechOpen, 2018, pp. 59−72.

[46] T. Mukherjee, S. Kambhampati, S. A. Morley, T. P. Durrett, and D. K. Allen, "Metabolic flux analysis to increase oil in seeds," *Plant Physiology*, vol. 197, no. 2, Feb. 2025, Art. no. kiae595, doi: 10.1093/plphys/kiae595.

[47] H. Zhao, D. K. Kosma, and S. Lu, "Functional role of long-chain acyl-CoA synthetases in plant development and stress responses," *Frontiers in Plant Science*, vol. 12, Mar. 2021, Art. no. 640996, doi: 10.3389/fpls.2021.640996.

[48] W. Aschariyaphotha, S. Noichinda, K. Bodhipadma, and C. Wongs-Aree, "Characterization of alcohol acetyltransferases in the ripe flesh of 'Monthong' and 'Chanthaburi 1′ durians," *Plant Physiology and Biochemistry*, vol. 206, Jan. 2024, Art. no. 108241, doi: 10.1016/j.plaphy.2023.108241.

[49] Y. Ueda et al., "Functional characteristics of aldehyde dehydrogenase and its involvement in aromatic volatile biosynthesis in postharvest banana ripening," *Foods*, vol. 11, no. 3, 2022, Art. no. 347, doi: 10.3390/foods11030347.

[50] L. Pei et al., "LOX and AAT genes affect the aroma of "Xiaobai" apricot during postharvest storage," *Food Processing and Preservation*, vol. 2023, 2023, Art. no. 5558605, doi: 10.1155/2023.5558605.

[51] F. Brian et al., "Ester content of blueberry fruit can be ruled by tailored controlled atmosphere storage management," *Postharvest Biology and Technology*, vol. 222, Apr. 2025, Art. no. 113355, doi: 10.1016/j.postharvbio.2024.113355.

[52] X. Zhu et al., "Low temperature storage reduces aroma-related volatiles production during shelf-life of banana fruit mainly by regulating key genes involved in volatile biosynthetic pathways," *Postharvest Biology and Technology*, vol. 146, pp. 68–78, Dec. 2018, doi: 10.1016/j.postharvbio.2018.08.015.

[53] D. Zhou, Q. Liu, C. Wu, T. Li, and K. Tu, "Characterization of soluble sugars, glycosidically bound and free volatiles in fresh-cut pineapple stored at different temperature," *Food Bioscience*, vol 43, Oct. 2021, Art. no. 101329, doi: 10.1016/j.fbio.2021.101329.

[54] P. Rey-Serra, M. Mnejja, and A. Monfort, "Inheritance of esters and other volatile compounds responsible for the fruity aroma in strawberry," *Frontier in Plant Science*, vol. 13, Aug. 2022, Art. no. 959155, doi: 10.3389/fpls.2022.959155.

[55] Y. Asikin et al., "Assessment of volatile characteristics of okinawan pineapple breeding lines by gas-chromatography–mass-spectrometry-based electronic nose profiling and odor activity value calculation," *Chemosensors*, vol. 11, no. 10, Sep. 2023, Art. no. 512, doi: 10.3390/chemosensors11100512.

[56] Y. Wang et al., "Lipid peroxidation and jasmonic acid involved in the development of soft-nose disorder in 'Keitt' mango during storage," *Horticultural Science and Biotechnology*, vol. 100, no. 2, pp. 255–264, Aug. 2024. doi: 10.1080/14620316.2024.2395288.

[57] P. Panpetch and S. Sirikantaramas, "Fruit ripening-associated leucylaminopeptidase with cysteinylglycine dipeptidase activity from durian suggests its involvement in glutathione recycling," *BMC Plant Biology*, vol. 21, Feb. 2021, Art. no. 69, doi: 10.1186/s12870-021-02845-6.

Supporting Information

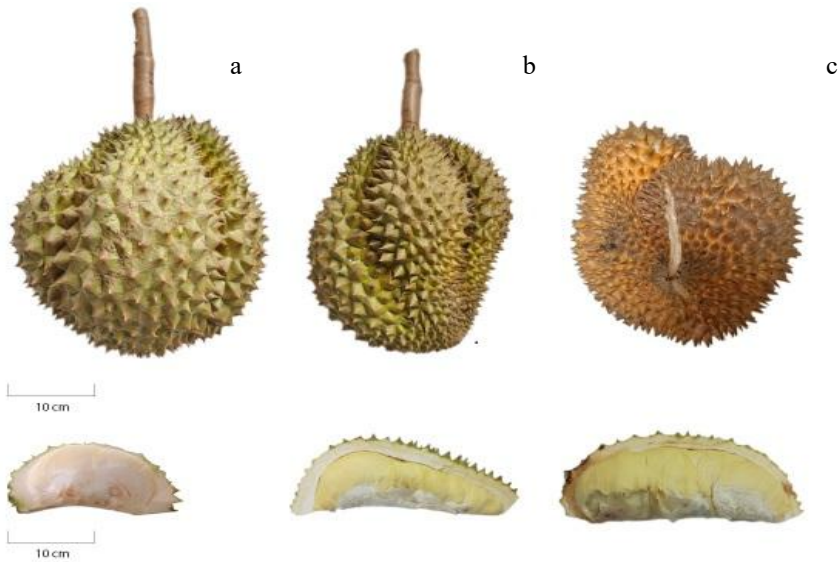

Figure S1: Characteristics of the fruit and pulp of 'Monthong' durian during 3 stages of ripening: Unripe durian (a) Ripe durian (b), Overripe durian (c).

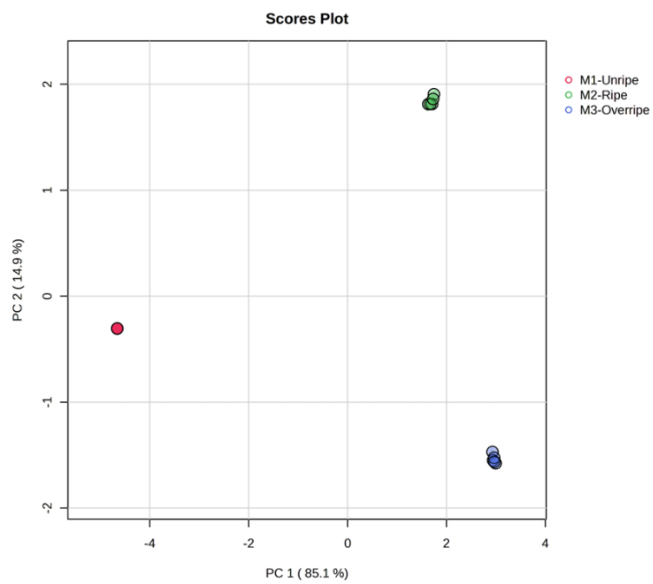

Figure S2: Principal Component Analysis (PCA) of volatile compounds in 'Monthong' durian at three ripening stages, based on OAVs.

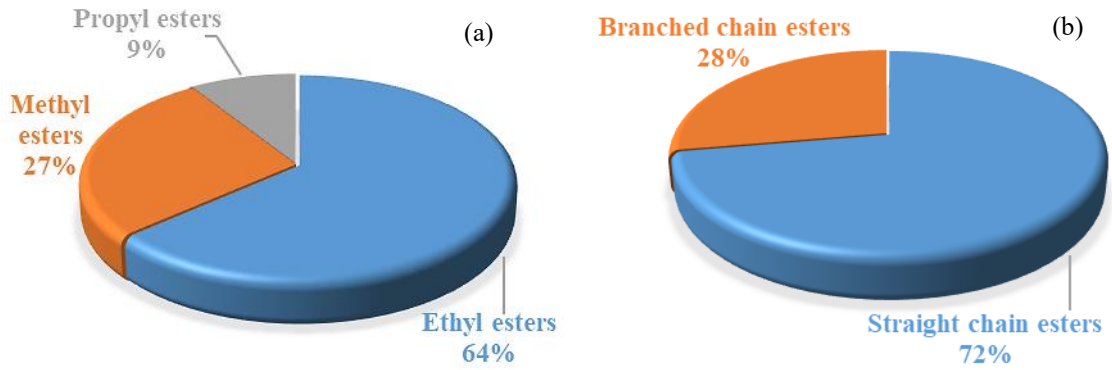

Figure S3: Portions of esters from different alcohols (a) and straight and branched chain esters (b) in ripe 'Monthong' durian pulp.